AFRL-AFOSR-VA-TR-2019-0197

A Cellworks Optimization Method for Air Vehicle Design

Marcelo Kobayashi
UNIVERSITY OF HAWAII SYSTEMS HONOLULU

05/31/2019
Final Report

Air Force Research Laboratory
AF Office Of Scientific Research (AFOSR)/ RTA1
Arlington, Virginia 22203
Air Force Materiel Command

REPORT DOCUMENTATION PAGE

Form Approved
OMB No. 0704-0188

1. REPORT DATE *(DD-MM-YYYY)*	2. REPORT TYPE	3. DATES COVERED *(From - To)*
	Final Report	3/1/2015 -n 2/28/2019

4. TITLE AND SUBTITLE
(HBCU) Collaborative Research: A Cellworks Optimization Method for Air Vehicle Design

5a. CONTRACT NUMBER
FA9550-15-1-0127

5b. GRANT NUMBER

5c. PROGRAM ELEMENT NUMBER

6. AUTHOR(S)
Kobayashi, Marcelo, H
Grandhi, Ramana, V

5d. PROJECT NUMBER

5e. TASK NUMBER

5f. WORK UNIT NUMBER

7. PERFORMING ORGANIZATION NAME(S) AND ADDRESS(ES)
University of Hawaii at Manoa, 2540 Dole Street, Holmes Hall 302
Honolulu, HI 96822
Wright State University, 210 Russ Engineering Center
Dayton, OH 45435

8. PERFORMING ORGANIZATION REPORT NUMBER

9. SPONSORING/MONITORING AGENCY NAME(S) AND ADDRESS(ES)
AFOSR
875 North Randolph Street, Suite 325
Arlington, VA 22203

10. SPONSOR/MONITOR'S ACRONYM(S)

11. SPONSOR/MONITOR'S REPORT NUMBER(S)

12. DISTRIBUTION/AVAILABILITY STATEMENT
Approved for public release; distribution unlimited

13. SUPPLEMENTARY NOTES

14. ABSTRACT
The primary objective of this research is the investigation of a biologically inspired methodology for the automated analysis and optimization of layout design. The problem can be multidisciplinary and involve multiple objectives, and can account for realistic engineering requirements. In aerospace systems development, there is a major gap in the number and types of configurations that are available between the conceptual and detailed design phases of vehicle development. This research introduced a framework which facilitates the availability of a large number of configurations by simultaneously performing size, shape and topology optimization

15. SUBJECT TERMS
Topology optimization, shape optimization, sizing, air vehicle design, map L systems, level sets, linear programing, non-linear programing

16. SECURITY CLASSIFICATION OF:			17. LIMITATION OF ABSTRACT	18. NUMBER OF PAGES	19a. NAME OF RESPONSIBLE PERSON
a. REPORT	b. ABSTRACT	c. THIS PAGE			Marcelo H. Kobayashi
					19b. TELEPHONE NUMBER *(Include area code)*
U	U	U	SAR	24	(808) 956-6579

(HBCU) Collaborative Research: A Cellworks Optimization Method for Air Vehicle Design

Final Performance Report
AFOSR Grant FA9550-15-1-0127

Marcelo H. Kobayashi, P.I.
Professor of Mechanical Engineering
University of Hawai'i at Manoa
2540 Dole Street—Holmes Hall 302
Honolulu, HI 96822
marcelok@hawaii.edu

Ramana V. Grandhi, Co-P.I.
Distinguished Professor of Mechanical and Materials Engineering
Wright State University
210 Russ Engineering Center
Dayton, OH 45435
ramana.grandhi@wright.edu

May 30, 2019

§1. OBJECTIVES

The primary objective of this research is the investigation of a biologically inspired methodology for the automated analysis and optimization of layout design. The problem can be multidisciplinary and involve multiple objectives, and can account for realistic engineering requirements.

In aerospace systems development, there is a major gap in the number and types of configurations that are available between the conceptual and detailed design phases of vehicle development. This research introduced a framework which facilitates the availability of a large number of configurations by simultaneously performing size, shape and topology optimizations during early stages of design.

§2. MAIN ACCOMPLISHMENTS

1. Integrated topology, shape and sizing optimization of trusses. For linear problems, i.e., those

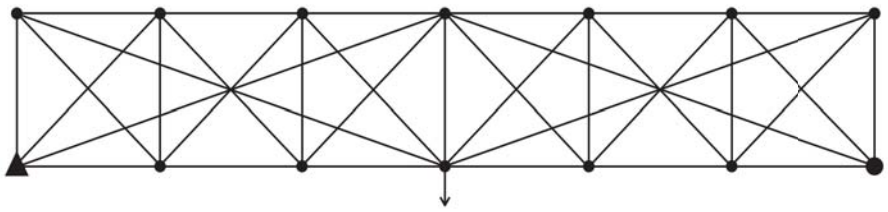

Figure 1: Possible ground structure for the problem of a one load span.

in which the objective function and constraints satisfy additivity[1] and homogeneity[2] with respect to their input, the optimization problem can be formulated as follows: find $\boldsymbol{x} \in \mathbb{R}^n$ that minimizes

$$\min_{\boldsymbol{x}\in\mathbb{R}^n} \quad \boldsymbol{c}^T\boldsymbol{x}, \tag{1}$$

subject to the linear constraints:

$$\boldsymbol{A}\boldsymbol{x} \leq \boldsymbol{b} \tag{2}$$

$$\boldsymbol{x} \geq 0 \tag{3}$$

where $\boldsymbol{c}^T$ is a covector of $\boldsymbol{x}$, and $\boldsymbol{A} : \mathbb{R}^n \to \mathbb{R}^m$ is a linear transformation on the admissible set of modulating variables with (possibly nill) image $\boldsymbol{b} \in \mathbb{R}^m$. Unless $m = n$, which guarantees a single solution for nonsingular $\boldsymbol{A}$, we expect non-unique solutions to this problem.

A ground structure is a predefined framework specifying both geometry (the positions of the nodes) and topology (member-node connectivities), which naturally restricts the allowed topologies of the optimized structure (see Fig. 1). Using a finite element discretization of a truss, the compliance optimization problem becomes a sizing problem for a fixed geometry:

$$\min_{\boldsymbol{a}\in\mathbb{R}^m,\boldsymbol{u}\in\mathbb{R}^n} \quad \boldsymbol{f}^T\boldsymbol{u} \tag{4}$$

$$\text{s.t.} \quad \boldsymbol{K}(\boldsymbol{a})\boldsymbol{u} = \boldsymbol{f} \tag{5}$$

$$\sum_{i=1}^{m} v_i = V \tag{6}$$

$$a_i \geq 0 \tag{7}$$

where $\boldsymbol{K}(\boldsymbol{a})$ is the reduced global structural stiffness shown explicitly as a function of the member areas. The problem consists of minimizing the compliance in terms of the design variables $\boldsymbol{a}$. According to the area bounds (7) the truss's topology is allowed to vary as a member's area may go to zero. V is a supplied upper bound on the total volume of the structure, and $v_i = a_i l_i$ is the ith member's volume defined by the product of its area,

[1] $f(u) + f(x) = f(u + x) \forall u, x \in S$

[2] $\alpha f(u) = f(\alpha u) \forall u \in S, \alpha \in \mathbb{R}$

a_i, with its length. If the global stiffness is written in terms of member volumes $\boldsymbol{K}(\boldsymbol{v})$, so $\boldsymbol{K}_i = \sum_{i=1}^{m} \frac{E_i}{l_i^2} \boldsymbol{\Gamma}_i \boldsymbol{\Gamma}_i^T$ the problem (2.9)-(2.12) is equivalent to a maximization in $\boldsymbol{u}$ subject to nonlinear constraints on the individual member strain energies

$$\max_{\boldsymbol{u} \in \mathbb{R}^n} \quad \boldsymbol{f}^T \boldsymbol{u} \tag{8}$$

$$\text{s.t.} \quad \boldsymbol{u}^T \boldsymbol{K}_i \boldsymbol{u} \leq 1 \tag{9}$$

where, for a positive semidefinite[3], symmetric $\boldsymbol{K}(\boldsymbol{v})$, which is the case, we can use the decomposition $\boldsymbol{u}\boldsymbol{K}_i\boldsymbol{u} = \left(\frac{\sqrt{E_i}}{l_i} \boldsymbol{\Gamma}_i^T \boldsymbol{u} \right)^2$ to arrive at a well-known **LP** formulation of the minimum compliance problems in terms of $\boldsymbol{u}$ alone:

$$\max_{\boldsymbol{u} \in \mathbb{R}^n} \quad \boldsymbol{f}^T \boldsymbol{u} \tag{10}$$

$$\text{s.t.} \quad -1 \leq \frac{\sqrt{E_i}}{l_i} \boldsymbol{\Gamma}_i^T \boldsymbol{u} \leq 1 \tag{11}$$

This problem admits an equivalent **LP** formulation in terms of slack variables $\boldsymbol{t}^{'}$ and $\boldsymbol{t}^{''}$

$$\min_{t^{'}, t^{''} \in \mathbb{R}^m} \quad \sum_{i=1}^{m} (t_i^{'} + t_i^{''}) l_i \tag{12}$$

$$\text{s.t.} \quad \sum_{i=1}^{m} \sigma_i (t_i^{''} - t_i^{'}) \boldsymbol{\Gamma}_i + \boldsymbol{f} = \boldsymbol{0} \tag{13}$$

$$t_i^{'}, t_i^{''} \geq 0 \tag{14}$$

where, if we make the substitution $t_i = \sqrt{E_i}(t_i^{''} - t_i^{'})$ for the ith member force and $a_i = (t_i^{'} + t_i^{''})$ for the corresponding member's area, we find that (2.15)-(2.16) is equivalent to a minimization of the volume, constrained by static requirements and stress conditions

$$\min_{\boldsymbol{a} \in \mathbb{R}^m} \quad \sum_{i=0}^{m} a_i l_i \tag{15}$$

$$\text{s.t.} \quad \sum_{i=0}^{m} t_i \boldsymbol{\Gamma}_i + \boldsymbol{f} = 0 \tag{16}$$

$$-\sigma_i a_i \leq t_i \leq \sigma_i a_i \tag{17}$$

[3]A matrix, $\boldsymbol{K}$, is positive definite if $\boldsymbol{x}^T \boldsymbol{K} \boldsymbol{x} > 0$ for all $\boldsymbol{x} \neq \boldsymbol{0}$. A positive semidefinite matrix is one which loosens the restriction on inequality to allow $\boldsymbol{x} = \boldsymbol{0}$.

which is Hemp's[4] linear programming formulation of Michell's problem with the scaling $\sigma_i = \sqrt{E_i}$. By duality in linear programming, a global optimum is guaranteed, though it need not be unique. This makes sense if we reflect that $\epsilon_i = l_i^{-1}\boldsymbol{\Gamma}_i^T\boldsymbol{u}$, so both of Michell's criteria are reflected in the dual formulations. Numerical solutions to **LP** are easily determined using Danzig's simplex algorithm. For example, applying **LP** to the ground structure in Fig. 1 gives the optimum shown in Fig. 2 with a volume $V_{LP} = 16.0$.

The next step is to extend the problem to an initial ground topology for which the spatial positions of the unrestrained nodes are allowed to vary. To this end, we consider the complete set of nodal coordinates in the non-reduced system. If $p \in \{1, ..., Nd\}$, corresponds to a possible degree of freedom the initial nodal positions can be collected in $\overline{\boldsymbol{y}} \in \mathbb{R}^{Nd}$. If $k \in \{1, ..., d\}$ the component $\overline{y}_p$ corresponds to the kth component of node j's position. Obtainable geometries are specified by a choice of a set $Y \subset \mathbb{R}^{Nd}$, such that $\boldsymbol{y} \in Y$ is a vector of allowed nodal positions. The problem can now be formulated as follows:

$$\min_{\boldsymbol{a}\in\mathbb{R}^m, \boldsymbol{u}\in\mathbb{R}^n, \boldsymbol{y}\in Y} \quad \boldsymbol{f}^T\boldsymbol{u} \tag{18}$$

$$\text{s.t.} \quad \boldsymbol{K}(\boldsymbol{a}, \boldsymbol{y})\boldsymbol{u} = \boldsymbol{f} \tag{19}$$

$$\sum_{i=1}^{m} a_i l_i(\boldsymbol{y}) = V \tag{20}$$

$$a_i \geq 0 \tag{21}$$

The admission of this nodal design variable affects the problem data in several ways, and may furnish added difficulty with regards to the phenomena of so-called 'melting nodes.' As the end nodes of a given member are varied the angle $\varphi_{i,k}(\boldsymbol{y})$, which member i makes with respect to axis k, changes. By this consideration so too does the direction cosine vector, $\Gamma_i(\boldsymbol{y})$. The individual member lengths are dependent on y in a more direct fashion, like

$$l_i(\boldsymbol{y}) = \sqrt{\sum_{k=1}^{d} \left(y_{\hat{\jmath}_{i,k}^{(target)}} - y_{\hat{\jmath}_{i,k}^{(source)}}\right)^2}$$

where two nodes are considered melting if $y_{\hat{\jmath}_{i,k}^{(source)}} = y_{\hat{\jmath}_{i,k}^{(target)}}$ $\forall k$, or $l_i(y) = 0$.

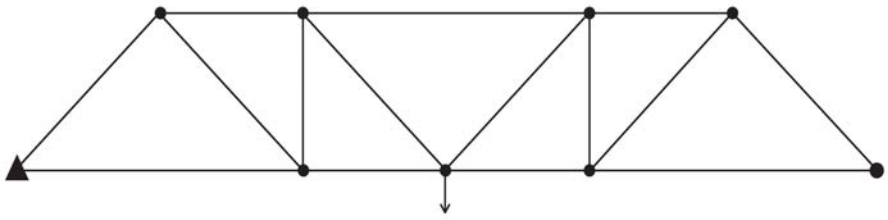

Figure 2: LP solution to the one load span using the ground structure in Fig 1.

[4]Hemp, WS, Optimum Structures, Clarendon Press, Oxford, 1973.

While the presence of melting nodes is crucial to limiting the number of bars, they may also form a singularity in the model, manifest in two ways: the function $l_i(\cdot)$ ceases to be differentiable for such geometries, and the global stiffness matrix becomes singular. To overcome these difficulties, Achtziger[5] provides an alternate evaluation for the functions $l_i(\cdot)$ and $K(\cdot,\cdot)$ as follows:

For each spatial dimension k, define a vector

$$\boldsymbol{v}_i^{(k)} \coloneqq [v_p^{(k)}]_i = \begin{cases} 1 & p = \hat{\jmath}_{i,k}^{(source)} \\ -1 & p = \hat{\jmath}_{i,k}^{(target)} \\ 0 & \text{else} \end{cases}$$

associated with the ith member whose Nd elements beget the matrix

$$\boldsymbol{C}_i \coloneqq \sum_{k=1}^{d} \boldsymbol{v}_i^{(k)} \big(\boldsymbol{v}_i^{(k)}\big)^T \tag{22}$$

where $\boldsymbol{C}_i \in \mathbb{R}^{Nd} \times \mathbb{R}^{Nd}$. The projection matrix, $\boldsymbol{P} \in \mathbb{R}^n \times \mathbb{R}^{Nd}$ is defined

$$\boldsymbol{P} = \Big(1_{n\times n}\ 0_{n\times s}\Big) \tag{23}$$

so that when it left multiplies a vector with Nd elements the first $p = 1, ..., n$ are retained, and the remaining, restrained degrees $p = n+1, ...Nd$ are nullified. In particular, these allow for the substitutions $l_i(\boldsymbol{y}) = \boldsymbol{y}^T\boldsymbol{C}_i\boldsymbol{y}$ and $\boldsymbol{\Gamma}_i = \frac{1}{l_i(\boldsymbol{y})}\boldsymbol{P}\boldsymbol{C}_i\boldsymbol{y}$. If a node melts we have $\boldsymbol{y}^T\boldsymbol{C}_i\boldsymbol{y} = 0$, which implies $\boldsymbol{C}_i\boldsymbol{y} = \boldsymbol{0}$. The denominator of $\boldsymbol{\Gamma}_i$ is addressed by a suitable change of variables.

Using similar manipulations to those yielding the linear programming problem **LP**, we arrive at a nonlinear programming (**NP**) form for simultaneous member size and truss shape optimization

$$\min_{\substack{\mu,\lambda\in R^m \\ y\in Y}} \quad \sum_{i=1}^{m} \big(t_i^{'} + t_i^{''}\big)\boldsymbol{y}^T\boldsymbol{C}_i\boldsymbol{y} \tag{24}$$

$$\text{s.t.} \quad \sum_{i=1}^{m} \sigma_i\big(t_i^{''} - t_i^{'}\big)\boldsymbol{P}\boldsymbol{C}_i\boldsymbol{y} + \boldsymbol{f} = \boldsymbol{0} \tag{25}$$

$$t_i^{'}, t_i^{''} \ \geq\ 0 \tag{26}$$

which is seen to be cubic in the objective function and quadratic in the dynamic constraints. If we reassert the change of variables $a_i = (t_i^{'} + t_i^{''})l_i(\boldsymbol{y})$ and $t_i = \sqrt{E_i}(t_i^{''} - t_i^{'})l_i(\boldsymbol{y})$ we recover a similar minimum volume problem. Approximate solutions satisfying the necessary first-order Karush-Kuhn-Tucker (KKT) conditions are readily found using the method of

[5] Achtziger, W. (2007). On simultaneous optimization of truss geometry and topology. Structural and Multidisciplinary Optimization, 33(4-5), 285-304.

sequential quadratic programing (SQP). Applying **NP** to the ground structure of Fig. 1 gives the framework in Fig. 3, which has a volume $V_{NP} = 9.6462$ and whose height is the same as the length of the mid span length, a.

The **LP**and **NP** problems provide efficient local optimizers. Given an initial ground structure, and constraints, the **LP** form guarantees a solution for both statically determinate and statically indeterminate truss structures. The existence of such solutions are, in part, due to a duality criterion in linear programming which stipulates that a solution to minimization problem is an optimum only if it is also the solution to a corresponding maximization problem, but more specifically through their satisfaction of Michell's criteria. If the problem is convex the global optimum is easily obtainable. Otherwise, one expects either non-unique solutions, say a minimum volume that is attainable by several layouts, or a multitude of local optima, or volumes, such that a global optimum is not readily discernible. The **NP** form provides a more robust search as concerns minimum volume trusses, allowing for the structure's geometry to be considered in concert with individual member sizing. As with the linear problem, various optima are attainable, each of which will typically satisfy the first order KKT conditions.

A restriction to either approach is that they can only loosely be interpreted as optimizing the topology—that is, by allowing members to vanish from the framework. Those members whose areas shrink to zero are eliminated from the structure, but are such that they may reappear, as required, to bear load. This is to say that an initial topology is defined for the structure such that the subsequent obtainable, or allowable, topologies are understood to be subsets of the original. For the nonlinear case, melting nodes provide another avenue for topology optimization, in particular individual members may vanish ($l_i = 0$) or reemerge ($l_i = 0 \rightarrow l_i \neq 0$). This annihilation, or generation, is restricted, however, because only those predefined members are allowed to participate in the design-space search.

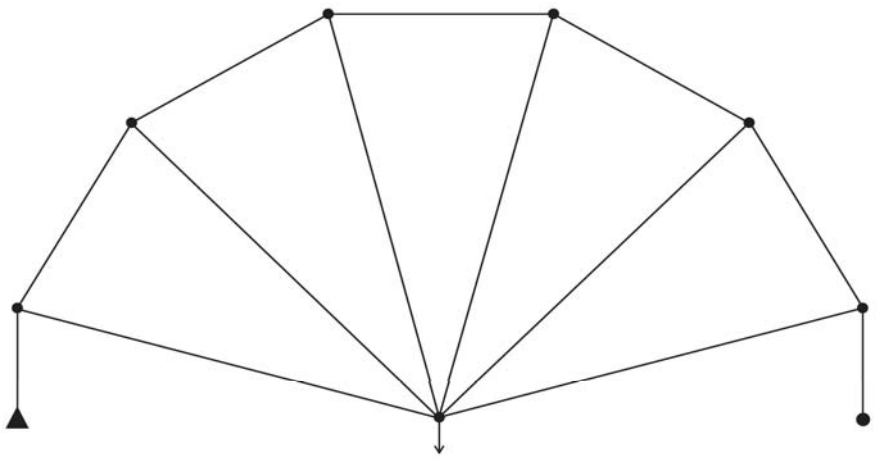

Figure 3: NP solution to the one load span using the ground structure in Fig. 1.

Either means of topology optimization (vanishing areas and melting nodes) suffer from the same limitation: they rely on a predefined topology, and therefore are limited in which optimum can ultimately be expressed. As per Michell's observation, an optimum framework is optimum only with respect to the set of possible frameworks considered. To determine the ideal structure we must consider all those structures satisfying the required equilibrium and stress constraints. In the continuum limit, the entire design space can be actualized. Such a structure would require members on the order of infintesimal lengths, which is impractical for actual truss constructions. Instead, one generally considers a finite, discretized search space: a ground structure. An increasingly dense and connected ground structure can approximate a continuous design space, yet the computational resources required to do so quickly becomes prohibitive. For example, analyzing a problem with twice the aspect ratio of a similar, original problem, would require at least twice as many design variables to maintain the same ground structure density. Generally speaking, a more refined ground structure will also produce an overabundance of redundant design variables, which can add undesired, unwarranted, complexity.

The proposed methodology seeks to avoid these shortcomings, providing a novel program for identifying optimal truss layouts—that is, simultaneous size, shape, and topology optimization, without the precondition of a ground structure. This approach works in tandem: a Genetic Algorithm[6] (**GA**) is encoded to explore pure topological information using the formalism of map L-systems and a subordinate program exploits this information and configures the trusses' geometry and material allocation according to **NP**. To start, we require a simply connected geometry of three or more line segments, termed the initial map in the sense of an L-system. This topological construct is discretized to be compatible with later geometric considerations and assumes that possible connections are realized by (straight) lines. Assigning to each edge a marked label from an alphabet, Σ, and an axiom, ω. By specifying a set of productions and applying them in parallel a given number of times we generate a novel topology from the initial map. In a post processing step the developed topology is provided a more specific geometry: map vertices become nodes and are given a location, and connections become members with determined length. This information is provided to the **NP** form and the optimum volume, if it exists, is approximated.

For the remainder, the initial map[7] is chosen such that predetermined vertices correspond to restraint and load sites in the problem. This need not be the case—various approaches can be employed to mobilize vertices in the bulk as support or load sites, either though direct implementation, or by exploiting the geometrical symmetries of a problem. Note that by specifying an initial we have not pre-determined those obtainable topologies; instead, this consideration influences the dynamics of cellular and evolutionary development[8]. Consequently, this map exists in a gradation between Michell's upper bound (a finite design space with finite boundary) and lower bound (an unbounded, continuous design space), as we can stretch and refine the topology as desired. It remains to determine, provided

[6] Goldberg, D. E. (2006). Genetic algorithms. Pearson Education India.

[7] Pedro, H. T. C., and Kobayashi, M. H. (2011). On a cellular division method for topology opti- mization. International Journal for Numerical Methods in Engineering, 88(11), 1175-1197.

[8] That is, how the topology grows over successive application of productions, and the paths investigated by the the coupled **GA**.

some map, which axiom and productions (which grammar) should be supplied to develop the topology of an optimum structure. In the sequel we will refer to this methodology as Evolutionary Programming **EP**, for brevity.

Genetic Implementation. We would like to optimize a truss problem (**TP**) with s supports and p applied loads. First, connect these by a convex polygon of degree at least $n \geq s+p \geq 3$ to construct a map ϖ. Set an alphabet $\Sigma \coloneqq \{\lambda, 0, ..., \eta_{nt} - 1\}$, where η_{nt} is a set number of non-terminal tokens. A trial candidate for $\mathbf{TP}_{\varpi}$ is constructed like

$$a^{\varpi}_{candidate} = [\eta_{dc}, \omega, P] \tag{27}$$

where η_{dc} is the number of developmental cycles, which are applications of the production rules. The axiom, $\omega \in \Sigma^*$, is generated by assigning a marked label to each of the maps edges taken from $\{0, ..., \eta_{nt}\}$. Production rules $P = [P_0, ..., P_{\eta_{nt}-1}]$ are like those described for map L-systems, and are applied to the axiom η_{dc} many times. Passing the resulting topology to **NP** yields an optimum volume $V^{\varpi}_{candidate}$ which is, for all intents, determined, up to the attainable minima of $\mathbf{TP}_{\varpi}$, according to $a^{\varpi}_{candidate}$. These genetic attributes are readily encoded in a binary string such as

$$a^{\varpi}_{candidate} = b_1^{(\eta_{dc})}...b_{\eta_1}^{(\eta_{dc})}b_1^{(\omega)}...b_{\eta_2}^{(\omega)}b_1^{(P)}...b_{\eta_3}^{(P)} \tag{28}$$

where η_{dc} is relegated to a $\eta_1 = 4$ bit representation, providing for (at most) seventeen developmental cycles. In other words, we consider $\eta_{dc} = (2 + (b_1...b_4)_2 \mathrm{mod}\ m_1)$ possible divisions, with $b_i \in \{0, 1\}$ and $1 \leq m_1 \leq (10000)_2 = 16$. A minimum $\eta_{dc} \geq 2$ is required so that progress is made away from the axiom; the maximum number is set by choosing a value $m_1 \in \mathbb{N}$ at most one greater than the maximum value expressed by η_1 bits. For example, if $m_1 = 3$ there are six ways to obtain $\eta_{dc} = 2$ and five to obtain $\eta_{dc} = 3$ or $\eta_{dc} = 4$. Depending on the level of refinement we might insist on a larger m_1, expanding the bit count as needed; that is, choosing $m_1 \geq 17$ has no effect for $\eta_1 = 4$. The axiom is stored in $\eta_2 = 17n$ bits, seventeen for each element, or label. Directionality $(\rightarrow, \leftarrow)$ is assigned to each label using the first entry, b_1, of the seventeen; the remaining bits set the edge label $(b_2...b_{17})_2 \mathrm{mod}\ \eta_{nt} \in \Sigma$. To each nonterminal we assign a production of the form

$$Y \rightarrow Z_1...Z_{m_2}$$

where $Y \in \Sigma_m$ is mapped to a sequence of Z_i, each denoted by a bit string $b_1...b_{m_3}$ representing either: a directed non-terminal $X_i \in \Sigma_m$, a terminal $x \in \Sigma$, the empty token λ, or a possible division site $[X_i]$. Observe the homology between biological optimization through cellular division and this parametrization for a truss layout. Organisms begin their development as single cells which develop to some characteristic topology according to biological processes that compile and execute the objectives encoded in DNA. In analogy to this encoding of developmental source over helical structures, the axiom wraps the initial map with directed labels from Σ (acting as the nucleotides) and is matured according to the productions, which are representative of those biological processes actualizing the primordial instructions in DNA; the resulting topology, as opposed to the driving biochemical mechanisms, being of import.

Such are the N_{pop} individuals considered by the **GA**, which are assigned a fitness value according to the volume determined from **NP**. In the processing of each fitness evaluation, the axiom is developed to its final state and the initial geometry is supplied. To avoid potential geometric instabilities a constrained Delaunay triangulation is employed to " shore up" the geometry. This operation takes an initial set of points with predefined edges, or regions, and triangulates (produces a grid of triangles) in such a way to maximize the minimal angle of the resulting regions. From an initial, randomly generated, pool of genetic information, the population is subjected to N_{gen} generations of competition according to the selection, crossover, and mutation. Selection is accomplished by the tournament method, which pits m_4 randomly determined individuals against each other until a set percentage of the future generations genetic inheritance is selected; the remaining individuals are chosen from the fittest (elite) of the current generation. A single point crossover, as described in the prequel, is used for mutation. After each crossover step a bit flip operator is applied to each daughter individual. As the name suggests, this operator produces a mutant by assigning to each bit in its binary representation a chance μ that it flips—that is, $0 \to 1$ or $1 \to 0$, and are applied to non-elite individuals.

Three structural benchmark problems are studies according to **LP**, **NP**, and **EP**. Aside

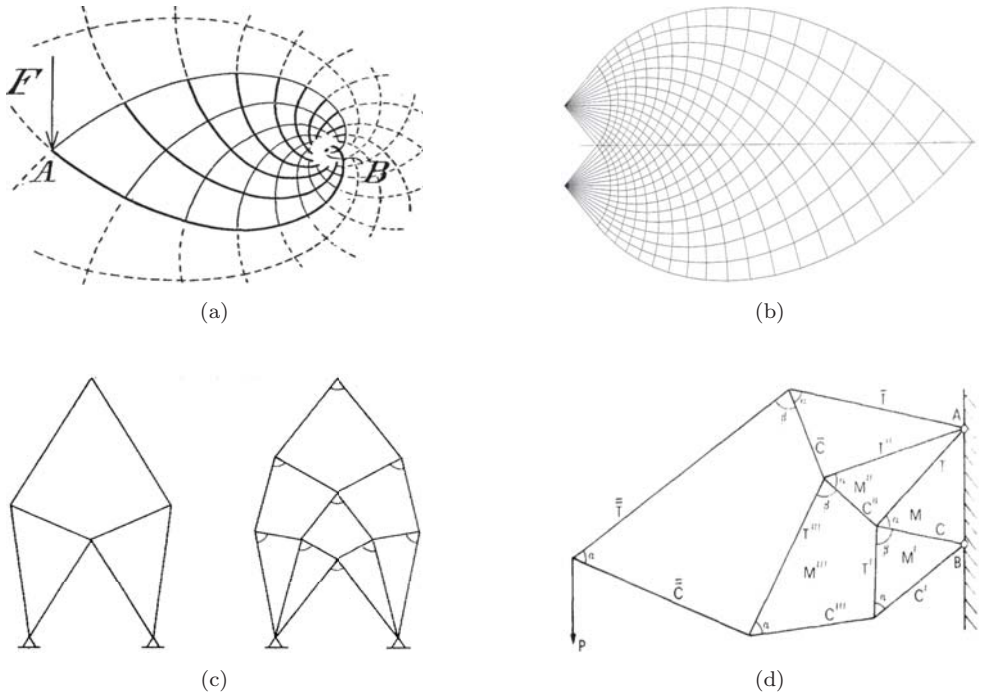

Figure 4: Michell optimum cantilevers: (a) the initial case presented by Michell with a single fixed support, (b) the variant solved by Chan with two fixed supports, and Prager cantilevers: (c) $N = 6$ (left) and $N = 11$ (right) node optima for a symmetric cantilever with two pinned supports and a single applied load, (d) optimum non-symmetric cantilever.

from Allison's results, we compare **EP** against the benchmark values generated by Achtziger[5] with the Sparse Nonlinear OPTimizer (SNOPT), an implementation of the SQP method developed by Gill et al.[9] that approximates the QP subproblem with a reduced-Hessian algorithm. The eigenresults were determined using SciPy's Sequential Least SQuares Programming (SLSQP) method, an SQP solver that replaces the quadratic subproblem with a linear least squares subproblem.

The first test case is a two load cantilever solved by Allison et al.[10] using a method differing from our own in several ways. Because minimum bounds are set on the attainable member areas the basic formulation requires a Sequential Linear Programming (SLP) solution and no global optimum is secured. It ignores direct geometry optimization, or variations of nodal positions, by choosing a parameter $C_{i,j} \in \{0, 1\}$ (i and j are two connected vertices) which removes bar $l_{i,j}$ from the system if $C_{i,j} = 0$, completely disregarding a vertex (node) if all members connected to it vanish. This should really be understood in the sense of mobilizing sub-topologies of the initial topology determined from $\omega_{\eta_{dc}}$ - solutions otherwise attained directly by application of **LP**, and thus not necessarily solutions which are optimum with respect to the geometry. To enforce geometric stability the initial map is chosen as a region connecting restrained and loaded joints, as ours, but is pre-divided into triangles. To maintain these triangular regions the allowed production divisions are restricted to compatible sites occurring adjacent to different vertices. A peculiarity in their formulation

$$\begin{aligned} \min_{\boldsymbol{A},\boldsymbol{C}} \quad & \sum \rho C_{i,j} A_{i,j} l_{i,j} \\ \text{s.t.} \quad & \sigma_{min} \leq \sigma_{i,j} \leq \sigma_{max} \end{aligned}$$

where ρ, $A_{i,j}$, and $l_{i,j}$ are the density, area and length of a member connecting nodes i to j, is the seeming lack of consideration for Newtons equilibrium criteria. It is indicated however, that (allowable) stresses are determined from member areas using the force method solved by SLP iteration.

The second test case is a finite variant of the optimum cantilever investigated by Michell in which a vertical load applied at a point A is ultimately supported by a force and couple acting on point B a horizontal distance AB from A. The resulting analytical, or Michell optimum, solution is given in Fig. 4a. Chan[11] considered a similar scenario: two pinned support aligned vertically to accommodate the lack of a flexural capacity in rods (Fig. 4b), albeit for limited aspect ratios. Observe that no moment is required, and that equilibrium is satisfied by a pair of equivalent forces, either acting on one or the other support. Lewinski et al.[12] extended these solutions to provide optima for all aspect ratios and load directions.

[9] Gill, P. E., Murray, W., and Saunders, M. A. (2005). SNOPT: An SQP algorithm for large-scale constrained optimization. SIAM review, 47(1), 99-131.

[10] Allison, J. T., Khetan, A., and Lohan, D. J. (2013, May). Managing variable-dimension structural optimization problems using generative algorithms. The Proceedings of the 10th World Congress on Structural and Multidisciplinary Optimization (WCSMO), Orlando, FL.

[11] Chan, A. S. L. (1960). The design of Michell optimum structures. College of Aeronautics Cranfield.

[12] Lewinski, T., Zhou, M., and Rozvany, G. I. N. (1994). Extended exact solutions for least-weight truss layouts, part I: cantilever with a horizontal axis of symmetry. International Journal of Mechanical Sciences,

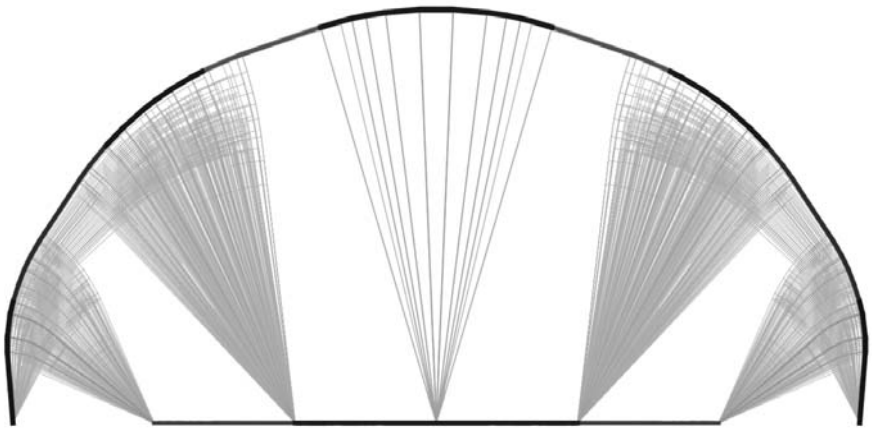

Figure 5: Optimum Michell framework for a span of five symmetric loads between two supports.

Of particular note is his recognition that Michell optima are arrived at by the limiting case of ideal (weightless) nodes, and that practical optima are determined respective to the node count of the finite structure. Prager[13] explored the finite limits of such frameworks using a circle of relative displacement, first for symmetric cantilevers, and later extending to the general finite cantilever with a single load and two vertically aligned supports. Of particular note is his recognition that Michell optima are arrived at by the limiting case of ideal (weightless) nodes, and that practical optima are determined respective to the node count of the finite structure.

The third test case is a five load bridge whose exact solution was provided only recently by Lewinski[14]. This result extends Michell's solution for a single load situated between two supports to an arbitrary number of evenly spaced loads. In total, these developments provide minimum bounds for the volumes of the examined frameworks, and suggest the topologies solutions might hope to attain.

Henceforth, all values are normalized and, as such, given without units to simplify the numerical treatment. Each force (member or applied) is taken proportional to a typical applied force F. The member stresses are taken against the stress bound σ, which is equivalent to setting $\sigma = 1$; their areas are non-dimensionalized by the ratio $\frac{F}{\sigma}$; their lengths are scaled by a typical length, l, and is enforced through the ground structure or initial map.

36(5), 375-398.

Lewinski, T., Zhou, M., and Rozvany, G. I. N. (1994). Extended exact least-weight truss layouts, part ii: Unsymmetric cantilevers. International journal of mechanical sciences, 36(5), 399-419.

[13] Prager, W. (1977). Optimal layout of cantilever trusses. Journal of Optimization Theory and Applications, 23(1), 111-117.

Prager, W. (1978). Nearly optimal design of trusses. Computers & Structures, 8(3-4), 451-454.

Prager, W. (1978). Optimal layout of trusses with finite numbers of joints. Journal of the Mechanics and Physics of Solids, 26(4), 241-250.

[14] Lewinski, T. (2018). Michell Structures. Springer.

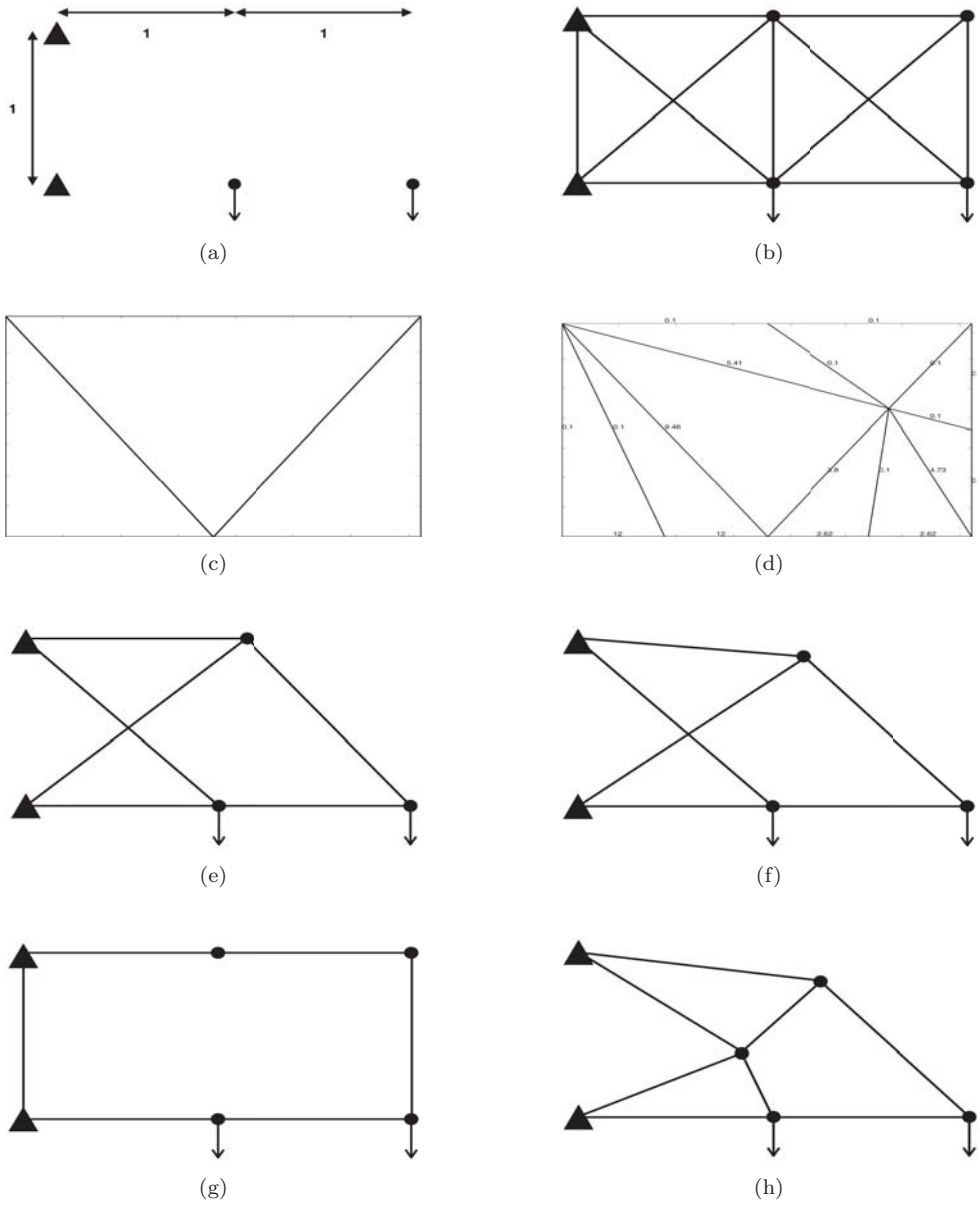

Figure 6: Two load non-symmetric cantilever: (a) the general structural scenario, (b) the ground structure used for the **LP** and **NP** solutions to the scenario, (c) the axiom used by Allison, (d) the optimum structure generated by Allison, (e) **LP** solution, (f) the **NP** solution, (g) the the initial map applied to conform with the load and restrain sites, (h) the **EP** solution.

and V by the quantity $\frac{Fl}{\sigma}$. A scaled Young's modulus, $E = 1$ is used, and $d = 2$ (as is the case for planar problems) for each.

The two load cantilever. We consider the scenario described in Fig. 6a of two vertically applied unit loads, one at coordinate (1,0) and the other at (2,0), and two pinned supports aligned vertically at (0,1) and (0,2). The ground structure consists of a 2×1 grid of $N = 6$ nodes (see Fig. 6b), each connected to its nearest neighbors for a total $m = 10$ potential members. The initial geometry is collected in the vector $\bar{\boldsymbol{y}} \in \mathbb{R}^{Nd}$, where $Nd = 12$. With two pinned supports there are $n = 2(6-2) = 8$ reduced global degrees of freedom, so $f \in \mathbb{R}^8$.

The optimum structure obtained by Allison using the initial map Fig 6c is the framework shown in Fig 6d, which obtains an actual volume of $V_{SLP} = 15880$ cu-in. Using the stress bound $\sigma = 25$ cu-in, the typical load $P = 100$ kip, and the typical length $L = 360$ in the volume normalized to $V_{SLP} = 11.03$. By (2.10)-(2.12) the **LP** solution $(\bar{\boldsymbol{t}}', \bar{\boldsymbol{t}}'') \in \mathbb{R}^{10}_+ \times \mathbb{R}^{10}_+$ gives the framework in Fig. 6e with an optimal, or minimal volume $V = 11.00$. To determine an **NP** solution, we stipulate the set of admissible geometries, $Y = \{\boldsymbol{y} \in \mathbb{R}^8 \mid y_p = \bar{y}_p \text{ for } p = n+1, ..., Nd\}$, and commence from the feasible point $(\bar{\boldsymbol{t}}', \bar{\boldsymbol{t}}'', \bar{\boldsymbol{y}})$ towards a KKT point, $(\boldsymbol{t}', \boldsymbol{t}'', \boldsymbol{y}) \in \mathbb{R}^{10}_+ \times \mathbb{R}^{10}_+ \times Y$. According to SLSQP the optimum volume in the nonlinear program is $V_{SLSQP} = 10.7952$. Starting from the initial map Fig. 6g **EP** determines the minimum structure Fig 6h with a a volume $V_{EP} = 10.3741$. This simple solution is 5.95% less than the Allison and **LP** minimums, and 3.90% less than the **NP** solution, which illustrates (in a small way) the gains attainable by **EP**.

The single load cantilever We turn to the scenario described in Fig. 7a of a vertically applied unit load load at coordinate (3,1), and three pinned supports aligned vertically at (0,1), (0,2), and (0,3). The topological domain consists of a 3×2 grid of $N = 12$ nodes (see Fig. 7b), each connected to its nearest neighbors for a total $m = 27$ potential members. The initial geometry is collected in the vector $\bar{\boldsymbol{y}} \in \mathbb{R}^{Nd}$, where $Nd = 24$. Given three pinned supports there are $n = 2(12-3) = 18$ reduced global degrees of freedom, so $f \in \mathbb{R}^{18}$.

The **LP** solution $(\bar{\boldsymbol{t}}', \bar{\boldsymbol{t}}'') \in \mathbb{R}^{27}_+ \times \mathbb{R}^{27}_+$ to this ground structure evidently yields a single framework (reflected in Fig. 7c&e) with an optimal, or minimal volume $V = 10$. We stipulate the set of admissible geometries, $Y = \{\boldsymbol{y} \in \mathbb{R}^{24} \mid y_p = \bar{y}_p \text{ for } p = n+1, ..., Nd\}$, and start from the linear solution $(\bar{\boldsymbol{t}}', \bar{\boldsymbol{t}}'', \bar{\boldsymbol{y}})$ towards the nonlinear solution $(\boldsymbol{t}', \boldsymbol{t}'', \boldsymbol{y}) \in \mathbb{R}^{27}_+ \times \mathbb{R}^{27}_+ \times Y$. The resulting solutions differ, with that from SNOPT (Fig. 7d) yielding a smaller optimal volume, $V_{SNOPT} = 9.114$, than that from SLSQP, $V_{SLSQP} = 9.133$, by approximately 0.2%. It is interesting that, where SLSQP converges to and terminates at Prager's symmetric $N = 6$ layout, SNOPT finds the same $N = 6$ solution in one iteration, yet continues to an optimum approaching, but not quite converging to, the symmetric $N = 11$ optimum. Inspecting the whole geometry, so both stressed and zero potential connections, it seems SLSQP only mobilizes nodes 2, 5, and 10; conversely, the sparse method fixes node 8 and varies the remaining free variables. Further numerical investigations reveal this topology is attained by SLSQP only for initial (feasible) geometries in a neighborhood of that optimum. Notice that the SNOPT result is not a simple truss, but produces a framework of intersecting members. The **EP** solution, initial map and structure in Figs. 7g&h, yields a

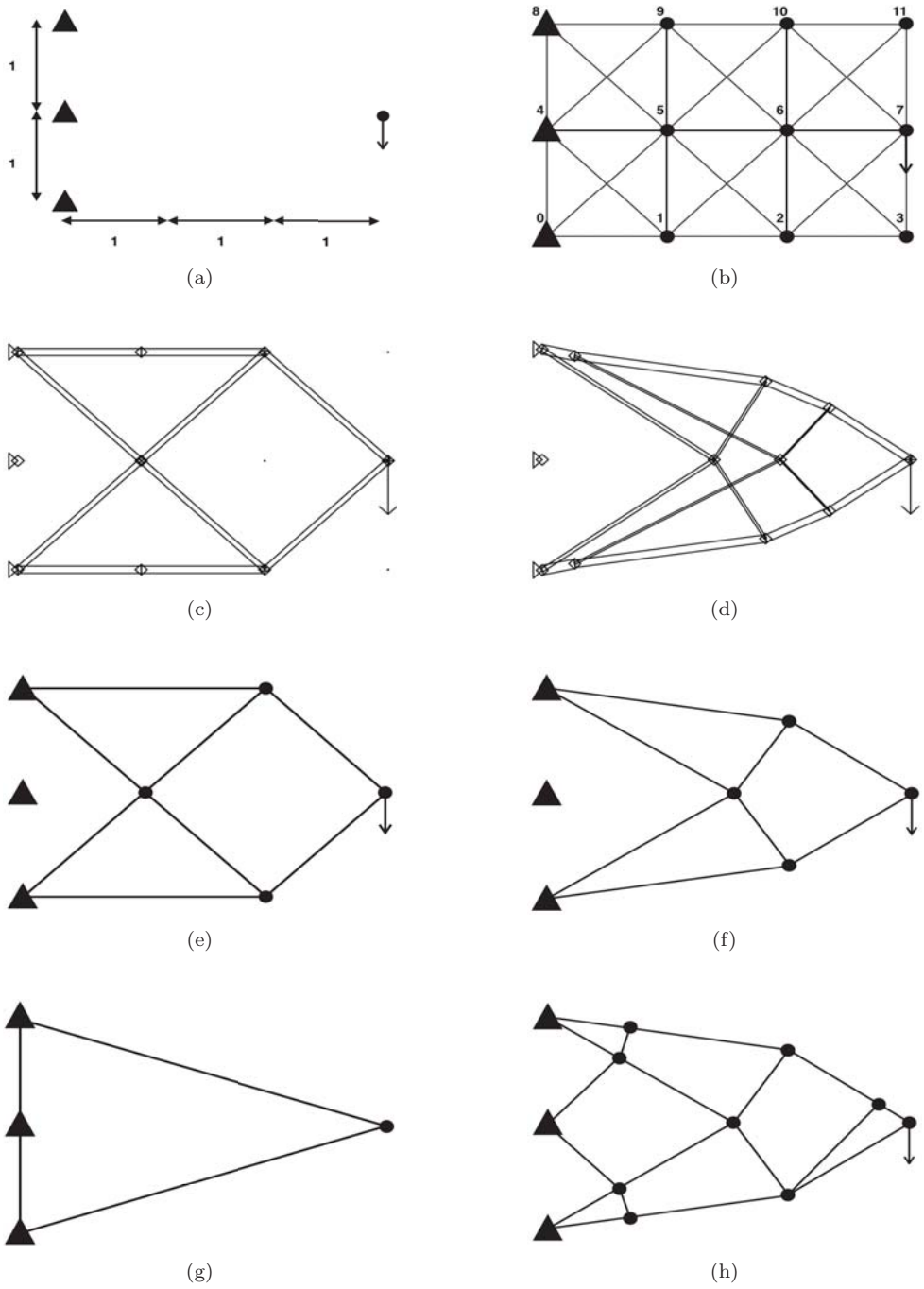

Figure 7: Single load symmetric cantilever: (a) the general structural scenario, aspect ratio 1.5, (b) the ground structure used for the **LP** and **NP** solutions to the scenario, (c) **LP** solution using SNOPT, (d) the **NP** solution using SNOPT, (e) the **LP** solution using SLSQP, (f) the **NP** solution using SLSQP, (g) the the initial map applied to conform with the load and restraint sites, (h) the **EP** solution.

volume $V_{EP} = 9.120$—less than SLSQP alone, but not as much as SNOPT.

The volumes obtained by all three methods agree[15] with the lower limit for a symmetric cantilever with 1.5 aspect ratio, $V_{cant,1.5} \approx 9$.

The five load span The next scenario (see Fig. 8a) entails a span of five unit loads evenly spaced on a unit interval between a pinned support (0,0), and a roller (6,0). The domain is set by $N = 12$ nodes arranged in a 6×1 grid (see Fig. 8b), each connected to its nearest neighbors for a total $m = 33$ potential members. The initial geometry is again collected in a vector $\bar{\boldsymbol{y}} \in \mathbb{R}^{24}$. For a single pinned support and roller there are $n = 2(12-1)-1 = 21$ reduced global degrees of freedom.

LP sizing provides a multitude of solutions $(\vec{\boldsymbol{t}}', \vec{\boldsymbol{t}}'') \in \mathbb{R}^{33} \times \mathbb{R}^{33}$ (two cases are shown in Fig. 8c&e), each with the same minimal volume, $V = 56$. For simultaneous sizing and geometry optimization we again stipulate the set of admissible geometries, $Y = \{\boldsymbol{y} \in \mathbb{R}^{24} \mid y_p = \bar{y}_p \text{ for } p = 22, ..., 24\}$, and embark from the linear solution. In contrast to the prior scenario, SLSQP yields a solution, $V_{SLSQP} = 34.9881$, which is marginally smaller than the SNOPT value, $V_{SNOPT} = 34.9924$. SLSQP generates a symmetric structure that seems a reasonable extension of the SNOPT estimate. The base geometry suggests this layout is arrived at by sliding node 9 away from 10, towards 8, which disengages member l_{39} and and activates l_{29}, forming the second triangle. Observe that the ground structure disallows topologies with five support triangles, and that both reproduce the vanishing bars l_{01} and l_{56}. The optimum solution generated by **EP**, the initial map and structure given in Figs. 8g&h, avoids these topological shortcomings, generating a symmetric framework in accords with Fig. 5 and a superior volume $V_{EP} = 34.6056$, about 1% lighter than either **NP** solution.

The volumes obtained by all three methods agree with the lower limit for a five load span with total length $L_{span} = 6$, that is $V_{span,5} = 34.2284$.

These results shows that the evolutionary programme introduced in this research topic successfully provides optimzed truss layouts—that is, sizing, geometry and topology optimization. The method performs, in the benchmark problems above, similarly or better than the best existing methods employing ground structures, and significantly better than those of Allison, which does not accomplish shape optimization. A journal paper is under preparation for this research topic.

2. Hybrid Cellular Division and Level Set Based Global-Local Design Framework for Structural Shape and Topology Optimization. This second research topic is similar to the previous one, but searches for more generic optimized structural frames as opposed to trusses, as in the first topic.

   In aerospace industries, the success of achieving a well developed vehicle that meets all the top level requirements needs high quality conceptual designs. Current early stage design procedures fail to yield a high number of configurations that could be further refined in

[15] For a given aspect ratio the optimum, non-dimensionalized volume is developed by an iterative scheme and plotted in [34]. Due to the quality of our copy, reading for 1.5 gives a volume between 8.8 and 9.0.

later stages of design. The challenges are due to lack of high fidelity simulations, integration of limited number of disciplines and more importantly lack of understanding of complex physics involved in that problem. The research in this topic introduces a new framework which facilitates the availability of a large number of configurations by simultaneously performing shape and topology optimizations during early stages of design. Cellular division

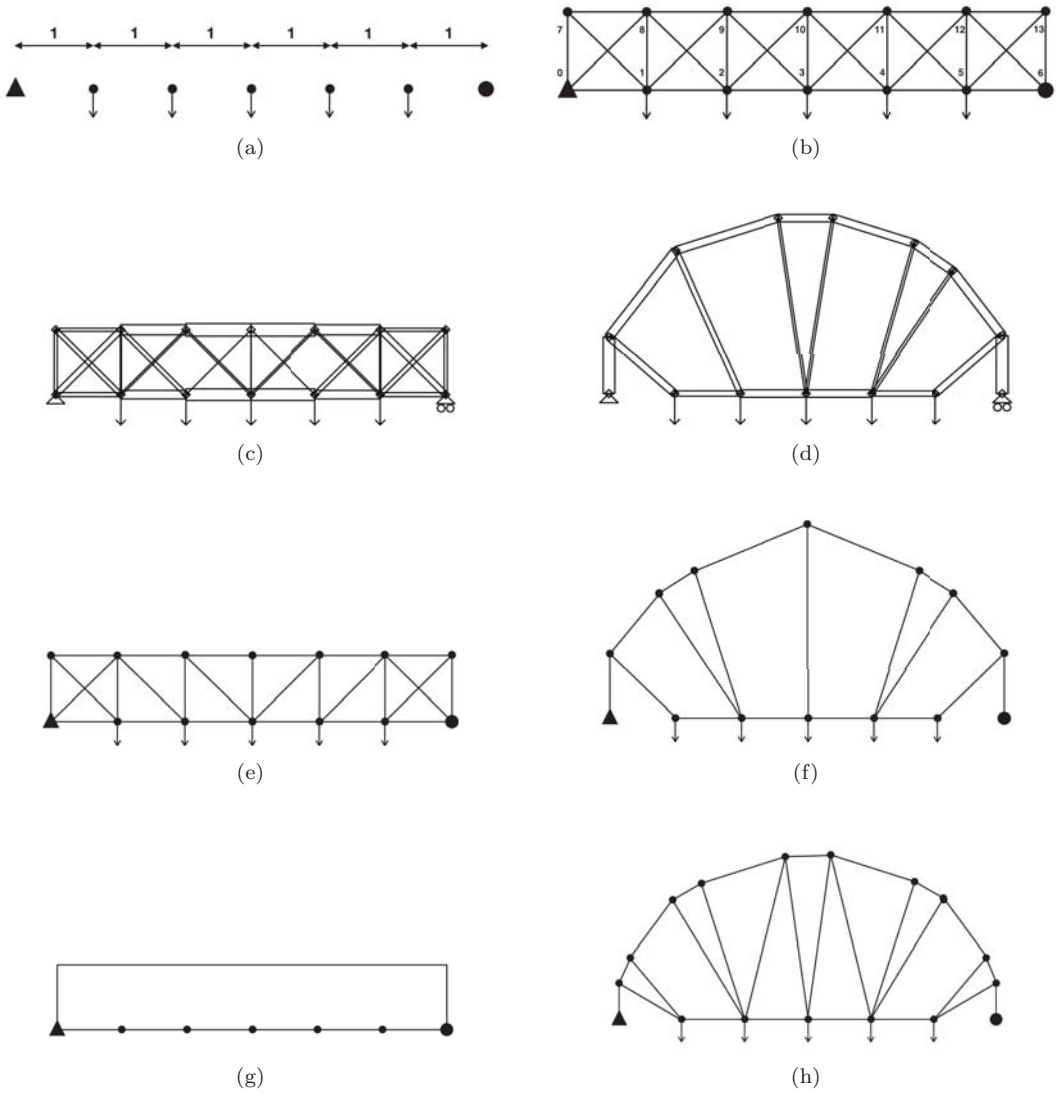

(a) (b)

(c) (d)

(e) (f)

(g) (h)

Figure 8: The five load span: (a) the general structural scenario, aspect ratio, (b) the ground structure used for the **LP** and **NP** solutions, (c) **LP** solution using SNOPT, (d) **NP** solution using SNOPT, (e) the **LP** solution using SLSQP, (f) the **NP** solution using SLSQP, (g) the the initial map applied to conform with the load and restrain sites, (h) the **EP** solution.

and level set based global-local optimization scheme is performed. Cellular division based design methodology is an innovative biologically-inspired layout and topology optimization method aimed at generating unconventional structural configurations by a global design space exploration. The approach facilitates creation of various designs that need further optimization to meet the multi-physics requirements. Level set method defines the structural boundary implicitly and optimizes based on the physical system behavior to handle designs with complicated shape changes, but it is highly dependent on its initial design choices. A combination of these two approaches with their individual strengths is synergistically integrated for evolving a globally optimized configuration from an open-ended design space. The new design framework was demonstrated on benchmark structural stiffness design problems and an aerospace application. Preliminary results of the research in this topic can be found in the conference papers:

- Hao Li, Ramana V. Grandhi and Marcelo H. Kobayashi (2018) "Level-set based cellular division method for structural shape and topology optimization," SciTech 2018, 2018 AIAA/ASCE/AHS/ASC Structures, Structural Dynamics, and Materials Conference, https://doi.org/10.2514/6.2018-1387, Kissimmee, FL 2018.
- Ramana V. Grandhi, Hao Li, Marcelo H. Kobayashi, and Raymond M. Kolonay "Vehicle Configuration Design using Cellular-Division and Level-Set Based Topology Optimization," EngOpt2018, 6th International Conference on Engineering Optimization, Lisbon, Portugal, 2018.

The final results of this research topic can be found in the upcoming journal paper:

- Hao Li, Ramana V. Grandhi, Marcelo H. Kobayashi and Raymond M. Kolonay (2019) "Hybrid Cellular Division and Level Set Based Global-Local Design Framework for Structural Shape and Topology Optimization," under review at Structural and Multidisciplinary Optimization.

3. Cellwork method. This third research topic seeks to extend the methodology above to three-dimensional layouts. As a first step in that direction, a novel cellwork L-system is introduced. The original cellwork L-system is characterized by the following[16]:

   - A finite set of cells, each cell surrounded by one or more faces.
   - Faces that are bounded by a finite, closed set of edges that meet at vertices.
   - Facets intersecting at edges, and edges crossing at vertices.

   These facets, edges and vertices must satisfy the following requirements:

   (a) Every facet is part of the boundary of a cell, and this boundary is connected.

   (b) There are no isolated vertices.

   (c) Every edge is a part of the boundary of a facet and this boundary is connected.

   The development of three dimensional layouts is modeled after a novel cellwork L system. Cellwork L systems are defined by an alphabet, Σ, an axiom, ω, and production rules P.

[16] Prusinkiewicz, P., and Lindenmayer, A. (2012). The algorithmic beauty of plants. Springer Science and Business Media.

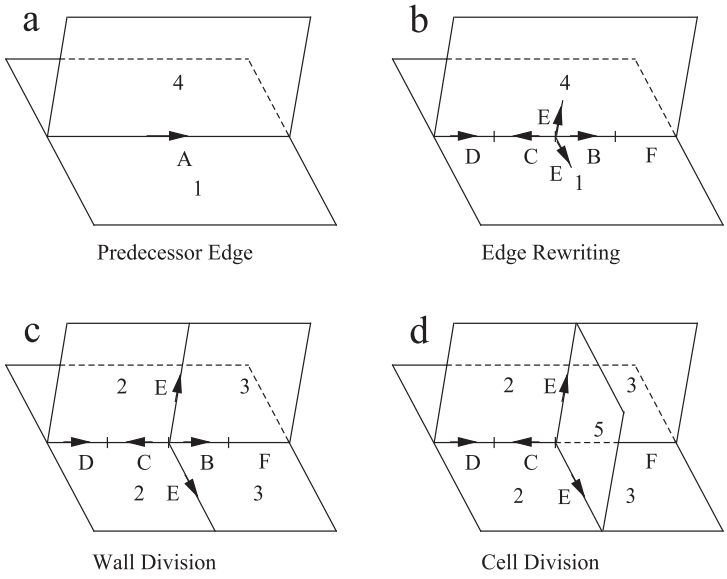

Figure 9: Phases of the derivation step

The alphabet provides labels for the edges and define other symbols that enters the cellular division. The axiom holds the labels of the edges of the initial cellwork. The production rules rewrite the edges and place the markers along the edges. For instance, the production

$$\vec{A} : 14 \rightarrow \vec{D}\vec{C}_2[\vec{E}_5]\vec{B}_3F$$

rewrites the edges in faces labeled 1 or 4 (see Fig. 9). It divides edges A in four and places a marker of type E in the faces 1 and 4. Markers on the same face with consistent orientation and that label the new face with the same letter are connected and the face is divided. The new faces are labeled according to the subscripts in the adjacent new edges (the new face containing the edge C is labeled 2, while the new face containing the edge B is labeled 3—see Fig. 9). If the new edges form a closed set and carry the same label, a new face is formed and the cell is divided. The new faces are labeled according to the subscripts in the adjacent new edges (the new face containing the edge C is labeled 2, while the new face containing the edge B is labeled 3i—see Fig. 9). If the new edges form a closed set and carry the same label, a new face is formed and the cell is divided.

In summary, the derivation step described above consists of three phases:

(a) Each edge of the cellwork is rewritten according to the corresponding production rule.

(b) Each face is scanned for matching markers. The first matching pair of markers that satisfies the criteria of face division (consistent orientation and face labeling) are connected and all remaining markers are discarded.

(c) Each cell is scanned for loops. If a loop is found with edges with the same label for the new face, then the new face is formed and the cell is divided along the new face.

The original cellwork L system can be used to model the development of interesting three dimensional biological layouts (see Fig. 10). However, two issues prevent its use for automatic layout generation: (1) the production rules can be ambiguous, and (2) the procedure do not specify the shape of new faces.

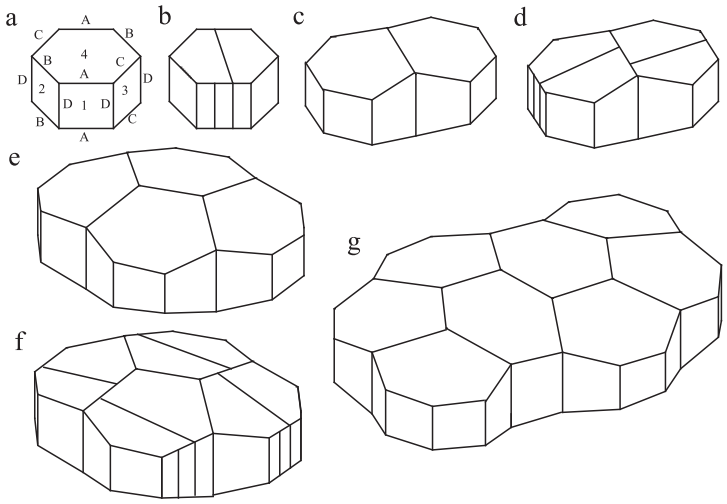

p_1 : A : 123 $\rightarrow$ $C_3[E_1]B_2[D_1]C_3$
p_2 : A : 4 $\rightarrow$ $CB_4[F_1]C_4$
p_3 : B : $*$ $\rightarrow$ A
p_4 : C : $*$ $\rightarrow$ B
p_5 : E : $*$ $\rightarrow$ D
p_6 : F : 123 $\rightarrow$ HGH
p_7 : F : 4 $\rightarrow$ $H_4[F_1]G_4[F_1]H_4$
p_8 : G : $*$ $\rightarrow$ F
p_9 : H : $*$ $\rightarrow$ G

Figure 10: Developmental sequence of a model of epidermal cells **?**

To understand how the production rules can be ambiguous, consider the following rules:

$$\overrightarrow{A} : 1 \rightarrow \overrightarrow{C}\overleftarrow{E}$$
$$\overrightarrow{A} : 2 \rightarrow \overrightarrow{A}\overrightarrow{B}$$

These rules are ambiguous since they specify two different divisions for the same edge.

Regarding the second issue, when a circular sequence of edges is found that is suitable for cellular division, the original method does not specify what surface to use.

The problem with the production rules is that they rewrite edges and the edges are the same entities regardless of the face they attached to. So for consistence, rules for different faces

can only differ in the markers they place at the different faces. We suggest the following variant for the production rules:

$$\vec{A} \to \vec{C}[_3\hat{F}_1][_6\overset{\vee}{D}_2]\vec{E}.$$

With this new production, the edge is always partitioned in the same way regardless of the faces adjacent to it—see figure 11. The markers now carry two face labels (the left and right subscripts), and an arrow head denoting its orientation ($\vee$, $\wedge$ denote a marker oriented towards or away from the juncture, respectively—this new notation for the marker orientation emphasizes the different orientations for the edges and the markers). The subscript at the right of the marker label denotes the face label where the marker can be inserted, whereas the left subscript denotes the label of the potential novel face: the source marker providing the label to the new face at the right of the new edge, while the target marker provides the label to the new face at the right of the new edge.

In this topic, the cellwork L system with the proposed production rules has been developed.

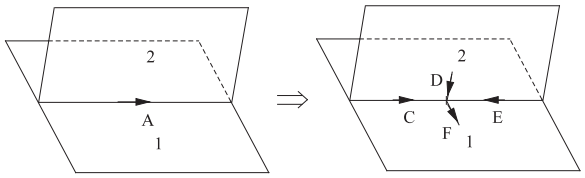

Figure 11: Example of consistent edge productions

Regarding the second topic, we establish that new faces are flat.

Currently, the cellworks L-systems outlined above has been implemented and tested. Two examples of layouts using the code are depicted below in Figs. 12 and 13. These results show that the cellworks L-systems can generate layouts for three-dimensional structural design.

4. Load paths in structural design. In this research topic, a load function method for load flow calculation in plane elasticity problems is pursued. The load functions are directly derived from 2D equilibrium equations. This research topic is motived by the in the previous topics and seeks for natural pathways for the load in space.

   The stresses are written in terms of the load functions and the load flow is calculated using the load function contours. The load functions are defined using generalized Beltrami representation. A constructive proof is given for the existence of load functions. A set of Poisson?s equations in terms of load functions and stress components are developed and an efficient numerical procedure to solve them is discussed. Numerical results show the proposed load function method is able to define the load paths and obtain the load flow using an Airy stress function for problems with available closed form solution, and also can be easily integrated into the numerical approaches to calculate load paths for complex problems. Details of the formulation can be found in the journal paper:

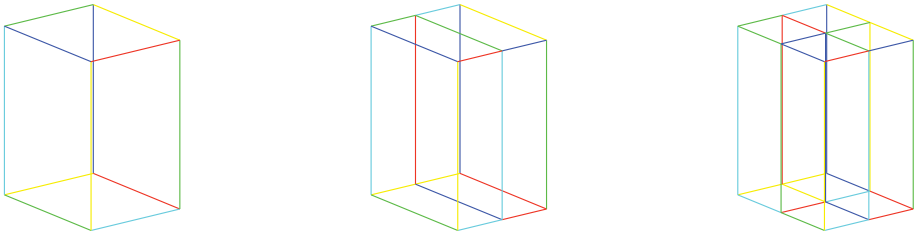

(a) cycle zero (b) cycle one (c) cycle two

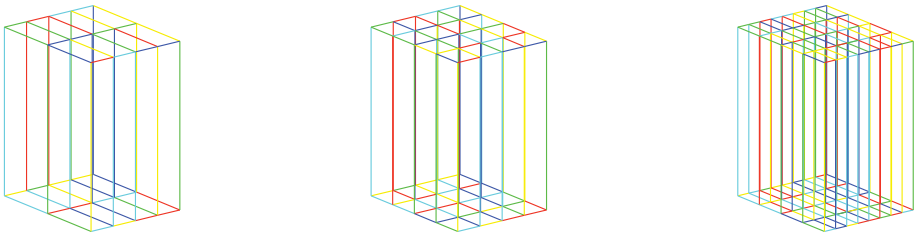

(d) cycle three (e) cycle four (f) cycle five

Figure 12: Cellworks example. Edge types are indicated with different colors.

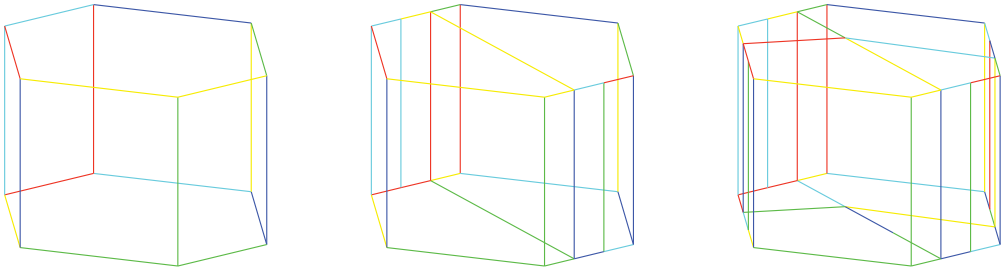

(a) cycle zero

(b) cycle one

(c) cycle two

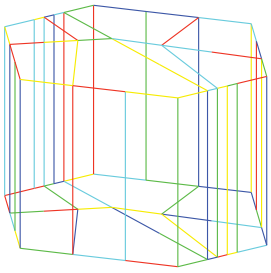

(d) cycle three

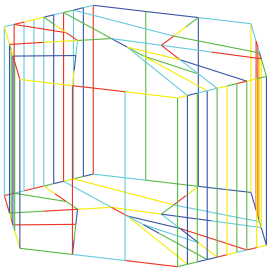

(e) cycle four

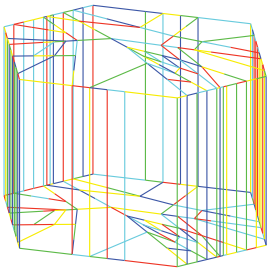

(f) cycle five

Figure 13: Cellworks example. Edge types are indicated with different colors.

- Ali Y. Tamijania, Kaveh Gharibia, Marcelo H. Kobayashi and Raymond M. Kolonay (2018) "Load paths visualization in plane elasticity using load function method," International Journal of Solids and Structures, Volume 135, 15 March 2018, Pages 99-109.

§3. PERSONNEL SUPPORTED

The grant supported the following personnel:

Faculty

1. M. H. Kobayashi, PI, Professor of Mechanical Engineering, University of Hawaii at Manoa.
2. R. V. Grandhi, Co-PI, Distinguished Professor of Mechanical and Materials Engineering, Wright State University.

Graduate Students

3. K. Hyun-eun, Ph.D., University of Hawaii at Manoa, Fall 2017-Spring 2018, advisor: M. H. Kobayashi[17].
4. H. Li, Ph.D., Wright State University, All But Dissertation, advisor: R. V. Grandhi.
5. V. Clark, M.Sc., University of Hawaii at Manoa, "On an Evolutionary Developmental Methodology for Pin-Joint Framework Optimization", defended Spring 2019, advisor: M.H. Kobayashi.

Research Experience for Undergraduate Students

6. Pookela Stillman Reyes, University of Hawaii at Manoa, advisor: M.H. Kobayashi.
7. Jeri Goodin, University of Hawaii at Manoa, advisor: M.H. Kobayashi.
8. Jaclyn Lee, University of Hawaii at Manoa, advisor: M.H. Kobayashi.
9. Irene Feng, University of Hawaii at Manoa, advisor: M.H. Kobayashi.
10. Tien Tran, University of Hawaii at Manoa, advisor: M.H. Kobayashi.
11. Adrian Ramirez, University of Hawaii at Manoa, advisor: M.H. Kobayashi.
12. Erik Lemasa, University of Hawaii at Manoa, advisor: M.H. Kobayashi.
13. Krystian Poland, University of Hawaii at Manoa, advisor: M.H. Kobayashi.
14. Igor Melnichenko, University of Hawaii at Manoa, advisor: M.H. Kobayashi.
15. Fabrice Rosala, University of Hawaii at Manoa, advisor: M.H. Kobayashi.
16. Raymond Andrade, University of Hawaii at Manoa, advisor: M.H. Kobayashi.

[17] For personal reasons, Mr. Hyun-eun dropped out of the Ph.D. program before its conclusion.

17. Dagan DeWeese, University of Hawaii at Manoa, advisor: M.H. Kobayashi.
18. Kai Outlaw-Spruell, University of Hawaii at Manoa, advisor: M.H. Kobayashi.
19. Alvin Yang, University of Hawaii at Manoa, advisor: M.H. Kobayashi.
20. Thomas Yang, University of Hawaii at Manoa, advisor: M.H. Kobayashi.

§4. PUBLICATIONS

The following publications acknowledge the support of this grant:

Journal

1. Ali Y. Tamijania, Kaveh Gharibia, Marcelo H. Kobayashi and Raymond M. Kolonay (2018) "Load paths visualization in plane elasticity using load function method," International Journal of Solids and Structures, Volume 135, 15 March 2018, Pages 99-109.
2. Hao Li, Ramana V. Grandhi, Marcelo H. Kobayashi and Raymond M. Kolonay (2019) "Hybrid Cellular Division and Level Set Based Global-Local Design Framework for Structural Shape and Topology Optimization," under review at Structural and Multidisciplinary Optimization.

Conference

1. Hao Li, Ramana V. Grandhi and Marcelo H. Kobayashi (2018) "Level-set based cellular division method for structural shape and topology optimization," SciTech 2018, 2018 AIAA/ASCE/AHS/ASC Structures, Structural Dynamics, and Materials Conference, https://doi.org/10.2514/6.2018-1387, Kissimmee, FL 2018.
2. Ramana V. Grandhi, Hao Li, Marcelo H. Kobayashi, and Raymond M. Kolonay "Vehicle Configuration Design using Cellular-Division and Level-Set Based Topology Optimization," EngOpt2018, 6th International Conference on Engineering Optimization, Lisbon, Portugal, 2018.

§5. INTERACTIONS

In the period of this grant, the following collaborations took place:

1. Ph.D. work of candidate H. Li. Dr. Ramana, as chair of the Ph.D. committee, and Dr. Kobayashi, as a member of the Ph.D. committee, have been collaborating on advising the Ph.D. work of candidate H. Li.
2. Visit to Wright-Patterson Air Force Research Laboratory from June 1 to June 30, 2018 for collaborative research with Dr. Kolonay.

§6. HONORS/AWARDS

1. Dr. Kobayashi was appointed Chair of the Department of Mechanical Engineering at the College of Engineering of the University of Hawaii at Manoa on July 1, 2017.
2. Wright-Patterson Air Force Research Laboratory (AFRL/RQ) 2019 Summer Faculty Fellowship Program.